ELSEVIER

Physics of the Earth and Planetary Interiors 120 (2000) 327–338

PHYSICS OF THE EARTH AND PLANETARY INTERIORS

www.elsevier.com/locate/pepi

The equation of state of $CaSiO_3$ perovskite to 108 GPa at 300 K

Sang-Heon Shim [a,*], Thomas S. Duffy [a], Guoyin Shen [b]

[a] *Department of Geosciences, Princeton University, Guyot Hall, Washington Road, Princeton, NJ 08544-1003, USA*
[b] *CARS, University of Chicago, Chicago, IL 60637, USA*

Received 13 December 1999; received in revised form 3 April 2000; accepted 3 April 2000

Abstract

Pressure–volume measurements have been performed for $CaSiO_3$ perovskite to 108 GPa at 300 K using NaCl and argon pressure-transmitting media, and energy dispersive X-ray diffraction (EDXD) in a diamond-anvil cell (DAC). By determining a parameter that is the product of the elastic anisotropy, *S*, and the uniaxial stress component, *t*, for each data point, we define the stress condition of the sample. For different points at the same pressure in a temperature-quenched sample, the *St* value can differ by as much as a factor of 5, indicating heterogeneity in the stress condition. This may be responsible for the large scatter of earlier *P–V* measurements in the DAC which in general used a large diameter X-ray beam. Also, the *St* value provides insight into the elastic anisotropy, *S*, of $CaSiO_3$ perovskite and platinum. The sign of *S* (positive) for $CaSiO_3$ perovskite agrees with first principles calculations but the magnitude may be inconsistent. A new compression curve at 300 K was obtained for $CaSiO_3$ perovskite by using those data points which represent the most nearly hydrostatic conditions. It is observed that the data points with high *St* values yield larger volumes than the points with small *St* values at a given pressure. By selecting the data points having low *St* values ($St \leq 0.005$), combining with lower pressure large volume press (LVP) measurements and fitting to third order Birch–Murnaghan equation of state (EOS), we find that $CaSiO_3$ perovskite is more compressible ($V_0 = 45.58 \pm 0.05$ Å^3, $K_{T0} = 236 \pm 4$ GPa, and $K'_{T0} = 3.9 \pm 0.2$ GPa) than suggested by previous studies. The density and bulk modulus of $CaSiO_3$ perovskite at lower mantle pressures and 300 K are 1–3% greater and 5–15% smaller, respectively, than found in previous studies. This study demonstrates that defining the stress state of the sample is crucial to obtain an accurate 300 K compression curve for unquenchable high-pressure phases.

Keywords: $CaSiO_3$ perovskite; Diamond anvil cell; Quasi-hydrostatic; Bulk modulus; Pressure derivative of bulk modulus

1. Introduction

$CaSiO_3$ perovskite is believed to be the major calcium silicate phase at lower mantle conditions. Liu and Ringwood (1975) first found that $CaSiO_3$ crystallizes in the perovskite structure at 16 GPa and 1800 K. The solubility of Ca in $MgSiO_3$ perovskite appears to be very small or negligible (Mao et al., 1977; Tamai and Yagi, 1989; Oguri et al., 1997; Hirose et al., 1999), which suggests that $CaSiO_3$ perovskite may exist as an independent phase in the lower mantle.

Since $CaSiO_3$ perovskite is not pressure quenchable, in situ measurement is the only available probe

* Corresponding author. Tel.: +1-609-258-3261; fax: +1-609-258-1274.
E-mail address: sangshim@princeton.edu (S.-H. Shim).

0031-9201/00/$ - see front matter
PII: S0031-9201(00)00154-0

to obtain information about the physical properties of this material. Static compression data for $CaSiO_3$ perovskite at ambient temperature have been reported across the entire lower mantle pressure range (24–135 GPa) in previous studies (Tamai and Yagi, 1989; Yagi et al., 1989; Tarrida and Richet, 1989; Mao et al., 1989). However, as discussed below, these results show a high degree of scatter which results in a range of fit values for the bulk modulus, K_{T0}, and especially poor constraints on the pressure derivative of the bulk modulus, K'_{T0}.

A possible explanation for this scatter could be non-hydrostatic stress conditions in the sample. However, the details of the stress condition were not quantitatively investigated in previous measurements. Furthermore, most of the earlier experiments were performed without using a pressure-transmitting medium. Thus, it is possible that the previous measurements are affected by non-hydrostatic stress. The resulting uncertainty in K_{T0} and K'_{T0} affects the accuracy of the 300 K isotherm. Shim and Duffy (2000) found that obtaining an accurate 300 K isotherm is particularly important for constraining the higher order thermoelastic parameters that are essential to deduce the physical properties of materials at extreme P–T conditions. Thus, it is necessary to more fully characterize the stress state of the sample and to develop an objective criterion to choose reliable P, V data points. We have performed P–V measurements to 108 GPa at ambient temperature for $CaSiO_3$ perovskite using either NaCl or argon as a pressure-transmitting medium. We also quantitatively analyze the stress conditions of the sample and apply this result to P–V equation of state (EOS) fitting.

2. Description of non-hydrostatic stress state

It has been shown that single-crystal elastic constants and the uniaxial stress component at high pressure can be obtained using X-ray diffraction (XRD) data measured under non-hydrostatic conditions (Singh et al., 1998; Mao et al., 1998; Duffy et al., 1999a,b). From the lattice strain theory for cubic crystals and assuming the isostress (Reuss) condition, the relative shift among different diffraction lines that results from uniaxial compression, such as occurs in a diamond-anvil cell (DAC) with a solid pressure medium, can be described as a function of the elastic anisotropy, S, the uniaxial stress component, t, the angle between the diffraction plane normal and load direction, ψ, and the Miller indices of the diffraction line, hkl (Singh, 1993):

$$\frac{a(hkl) - a(hkl^*)}{a_0} = -St(1 - 3\cos^2\psi)(\Gamma(hkl) - \Gamma(hkl^*)). \quad (1)$$

where $a(hkl)$ is the calculated unit-cell parameter from a single diffraction line, and the superscript * denotes a reference diffraction line (in this study, the 200 line was used for both materials under consideration, $CaSiO_3$ perovskite and platinum) and the subscript 0 denotes ambient conditions. As discussed elsewhere (Singh, 1993; Singh et al., 1998), the angle ψ is typically $\sim 85°$ in a DAC experiment, near 0° in a typical large volume press (LVP) experiment, and ψ can be varied continuously between 0° to 90° in a radial or side diffraction experiment in the DAC.

The uniaxial stress component, t, is defined as the difference between the principal stress along the axial direction of the DAC, σ_3, and the principal stress along the radial direction of the DAC, σ_1:

$$t = \sigma_3 - \sigma_1. \quad (2)$$

with t taken to be positive on compression. The elastic anisotropy factor, S, is given by,

$$S = s_{11} - s_{12} - \frac{s_{44}}{2}, \quad (3)$$

where the s_{ij}'s are the single-crystal elastic compliances. The parameter S can be either positive or negative and is zero for an elastically isotropic material. $\Gamma(hkl)$ is given by:

$$\Gamma(hkl) = \frac{h^2k^2 + k^2l^2 + l^2h^2}{(h^2 + k^2 + l^2)^2}. \quad (4)$$

By fitting the $(\Gamma(hkl) - \Gamma(hkl^*), [a(hkl) - a(hkl^*)]/a_0)$ data set to a linear equation (Eq. (1)), one obtains a slope that is equal to $-St(1–3\cos^2\psi)$. Since ψ is fixed for energy dispersive X-ray diffraction (EDXD), one can calculate the uniaxial

stress component if S is known. For platinum, S is equal to 0.0031 GPa^{-1} at ambient pressure (Macfarlane and Rayne, 1965) but its pressure dependence is unknown. In general, S may vary with pressure (Duffy et al., 1995). In the case of $CaSiO_3$ perovskite, only theoretical elastic constants are available for calculation of S (Karki and Crain, 1998). This result suggests that S is positive and decreases with compression from 0.0028 GPa^{-1} at 1 bar to 0.0002 GPa^{-1} at 120 GPa. Due to the uncertainty in S for these materials, we will use the product St as an indicator of the magnitude of the uniaxial stress component in a sample.

3. Experimental methods

A natural wollastonite from Newburg, NY was used as starting material. The crystallinity and purity were checked by XRD and energy dispersive spectroscopy (EDS). Minor amounts of Fe, Mg, and Mn were detected. However, the content of these impurities were always no more than the detection limit of the EDS technique (less than 1 mol%).

Powdered (≤ 5 μm) wollastonite was mixed with 10 wt.% platinum (grain size ≤ 1 μm) which served as a laser absorber and internal pressure standard (using the EOS of Holmes et al., 1989). 10-μm thick and 130-μm diameter foils were made from the $Pt + CaSiO_3$ perovskite mixture. These foils were loaded in a 150-μm diameter hole in a stainless steal gasket. Diamond anvils with a 300-μm flat culet were used at pressures below 70 GPa. At higher pressures, a 40-μm diameter foil was loaded in 50-μm rhenium gasket hole and compressed between a pair of beveled anvils with a 100-μm diameter central flat. NaCl or argon was also loaded as a pressure-transmitting media and served to insulate the sample from the diamond anvils. To prevent contact between the sample foil and diamond, we put small chips of starting material (wollastonite) between the sample and diamond. This also enables argon to flow between sample and diamond such that argon surrounds the sample and plays a role as insulator at high temperature.

The EDXD spectra were measured using a tapered undulator synchrotron source at the GSECARS sector (13-ID-D) of the Advanced Photon Source (APS) (Rivers et al., 1998). A 10×10 μm beam size was obtained using tungsten carbide slits. By measuring the XRD spectra over this small area, the effect of inhomogeneity due to stress gradients is expected to be reduced. Furthermore, the small beam size is useful to probe the stress condition around the heated area.

To transform lower pressure phases to the perovskite phase and to attempt to relax the deviatoric stress, the samples were heated ($T = 1500$–2400 K) at frequent intervals using the double-sided laser-

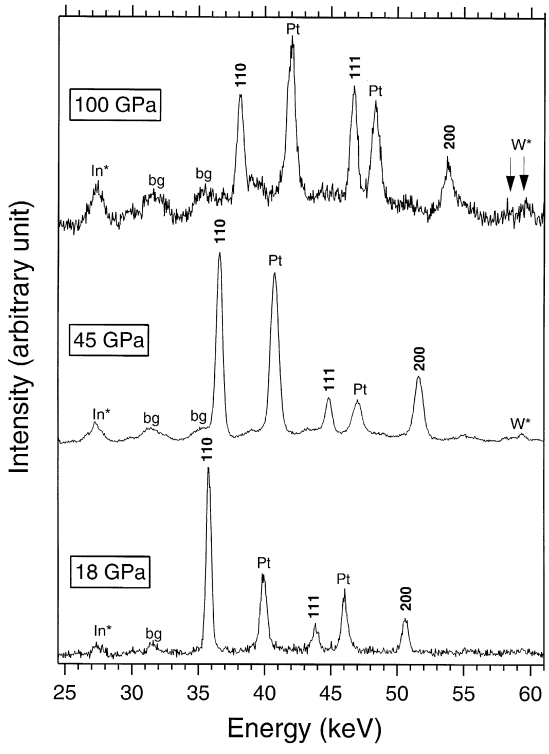

Fig. 1. Representative XRD patterns of $CaSiO_3$ perovskite at high pressures and ambient temperature. $CaSiO_3$ perovskite lines are indicated with (hkl) values. The background structure from the undulator insertion device is indicated by ''bg''. Indium and tungsten X-ray fluorescence lines arising from laser and X-ray optics, respectively, are marked. Pt indicates platinum diffraction lines. Although in these patterns the diffraction peaks from pressure medium (argon) are not clearly observed, other XRD patterns do contain peaks of the pressure medium and we also observe a transparent portion of the sample chamber which indicates the existence of transparent argon (sample mixture is dark gray due to platinum). During heating argon peaks tend to grow strongly, and the local variation of argon peak intensity is due to preferred orientation.

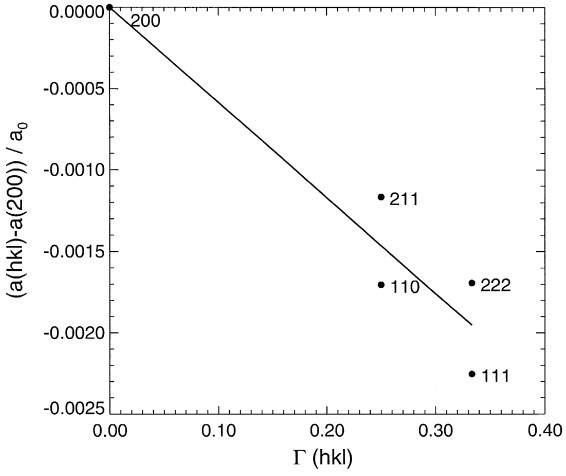

Fig. 2. Fit of the unit-cell parameter of $CaSiO_3$ perovskite from individual diffraction lines to Eq. (1). The *St* value is related to the negative of the slope. The Miller index of each point is shown at the right of the symbol. For this case, *St* was determined to be 0.0059 ± 0.0004.

heated diamond-anvil cell (DSLHDAC) technique (Shen et al., 1998). The $CaSiO_3$ perovskite phase begins to form during or after heating above 1000 K at more than 15 GPa (Shim et al., 2000). The XRD patterns at 300 K were measured up to 108 GPa (Fig. 1).

The XRD peaks were fit using a pseudovoigt profile function. The unit-cell parameters and volumes were calculated using four or more diffraction lines for $CaSiO_3$ perovskite and three or more for platinum. The *St* values were obtained for both materials by fitting the calculated unit-cell parameters from individual diffraction lines and their Miller indices to Eq. (1) (Fig. 2). For $CaSiO_3$ perovskite, we used at least three diffraction lines for the *St* calculation. Since we have two strong diffraction lines for platinum and the others are relatively weak, we used only the 111 and 200 lines to obtain the *St* value for platinum.

4. Results

4.1. Stress state of temperature-quenched samples

It has long been recognized that the uniaxial nature of the DAC could result in generation of significant non-hydrostatic stresses in a solid and produce a systematic error in P–V measurements (e.g., Kinsland and Bassett, 1977). By measuring the XRD pattern as a function of angle from the maximum stress direction of a DAC, Duffy et al. (1999a) confirmed that the measurement along the maximum stress direction could result in 30% overestimation of bulk modulus, K_0, in the case of rhenium. Although rhenium is extreme due to its large strength, this observation emphasizes the importance of quasi-hydrostatic conditions for P–V measurements or, at least monitoring the stress state of the sample.

In most of our XRD spectra, the 200 lines of $CaSiO_3$ perovskite and platinum yield larger unit-cell parameters than other lines (0.36% larger for $CaSiO_3$ perovskite on average). This was also observed for platinum and gold at high pressure and 300 K (Shim and Duffy, unpublished data). For gold, in side diffraction experiments, Duffy et al. (1999a) observed that the unit-cell parameter calculated from the 200 line is always higher than those from other lines for $\psi = 90°$ which is nearly the same condition as this study. They showed that this relative shift of the 200 line can be interpreted as a result of non-hydrostatic stresses in the sample for the case where $S > 0$.

In order to describe the stress state of the sample, we calculated *St* values for $CaSiO_3$ perovskite and platinum (Fig. 3). The *St* values for both $CaSiO_3$ perovskite and platinum show considerable scatter even at the same pressure. The *St* values are based on small shifts of diffraction lines (typically $\leq$ 0.7%), so part of this scatter may be caused by the low resolution of EDXD technique.

However, when diffraction patterns are recorded directly at high temperature (Shim et al., 2000), the scatter of *St* values decreases markedly and the average values approach zero. This means that the noise contribution from EDXD is small. This is consistent with the results of EDXD experiments on MgO under quasi-hydrostatic conditions (helium pressure-transmitting medium) in which mean lattice parameter differences from different diffraction lines were found to be only 0.03% (Speziale et al., 2000). Since S is constant for a given pressure and temperature, the observed scatter at 300 K must be caused by differences in t, i.e., heterogeneity in the sample stress state. To confirm this hypothesis, we probed

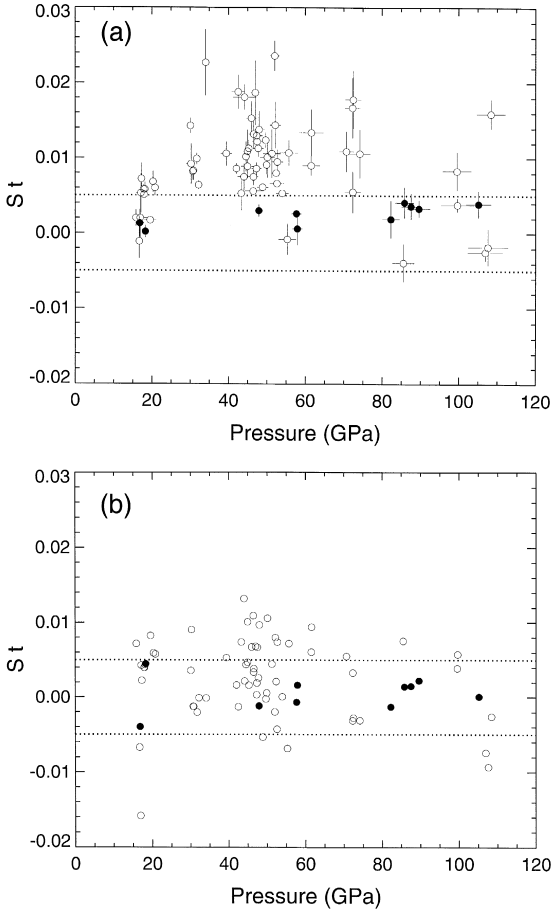

Fig. 3. Measured *St* values for (a) $CaSiO_3$ perovskite and (b) platinum versus pressure at 300 K. The data points with solid symbols are the points for which *St* of both $CaSiO_3$ perovskite and platinum are less than 0.005. These points were selected for EOS fitting. The estimated error (1σ) obtained from linear fitting is denoted by the error bar. Since only two diffraction lines were used, an estimated error is not available for platinum.

several spots near the heated area both after quench and cold compression (Fig. 4). This was possible by using a small X-ray beam of 10×10 μm. We obtained three or four spectra by shifting the sample relative to the incident X-ray beam by 10–15 μm in two orthogonal directions. Directly after temperature quench we typically found different *St* values at different positions from the heated spot (Fig. 4a). For the case of Fig. 4a, the measured pressure difference within a 30-μm area is no more than 2 GPa. In previous EOS studies of temperature-quenched high-pressure phases, a small radial pressure gradient was used to suggest that the sample is fully relaxed and deviatoric stress is not significant. However, the *St* measurement is a more direct probe of the stress state.

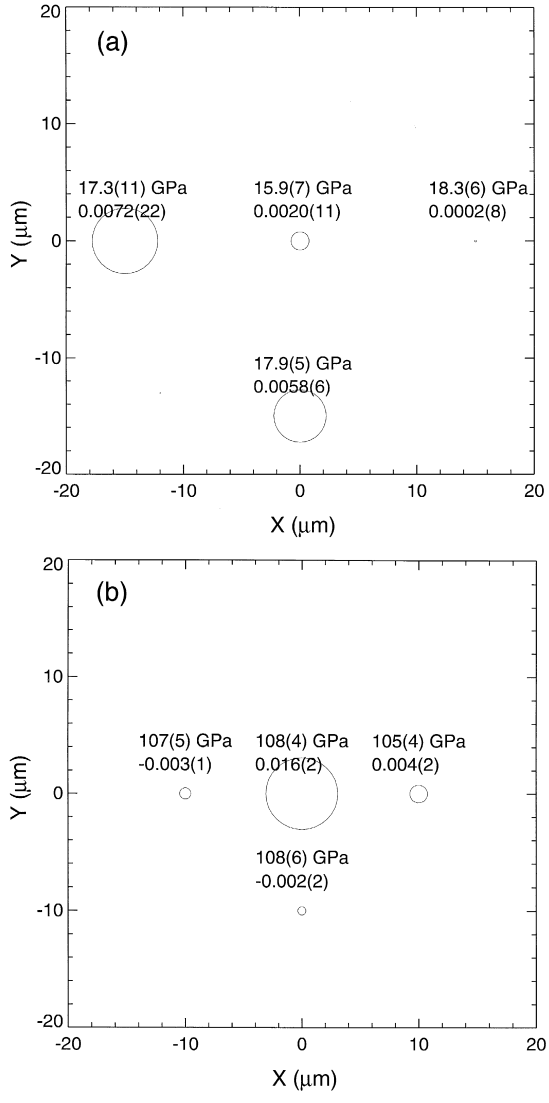

Fig. 4. Pressure and uniaxial stress component around the heated area (a) after quench and (b) after heating followed by compression at 300 K. The *X*- and *Y*-axes are the distances from the central heated spot. The size of symbol is proportional to the magnitude of the *St* value (the scale is different for (a) and (b)). For each point, the pressure and the *St* values are given above. The number in parenthesis is the estimated uncertainty (1σ).

The *St* value directly at the heated area is generally smaller than at surrounding areas, although not always the minimum as shown in Fig. 4a. This is consistent with the expectation that heating will release deviatoric stresses. However, after further cold compression, the heated spot does not have a smaller *St* value than surrounding areas any more (Fig. 4b). This indicates that heating the sample after compression as used by some earlier studies (Yagi et al., 1989; Mao et al., 1989) may be an effective way to reduce the differential stress.

As shown in Fig. 4, the *St* value varies dramatically over short distances near the heated area. We used a laser beam with a 40-μm diameter to heat the sample. The shape of the emitted intensity and temperature profiles are approximately Gaussian, although a TEM_{01} mode is used for heating. Thus, for the area within ± 10 μm from the center of the heated spot, the intensity and temperature profiles are nearly flat (Shim et al., 2000), and for the rest of the heated area the intensity and temperature decrease rapidly with a gradient of ~ 100 K/μm. Thus, the spot 15 μm away from the center corresponds to the position where thermal gradient becomes large. This different heating condition may be responsible for the observed inhomogeneity of *St* values within a small area (Fig. 4a). This problem worsens when we compress the material at 300 K after quench (Fig. 4b). In this case, at the center, the *St* value reaches a maximum. However, 10 μm away from the center, *St* is very close to zero. Again, this shows the heterogeneity of the stress condition within a small range. As pointed out previously, the pressures are nearly the same for the different spots within the experimental error range. Since, *S* is a function of pressure, we can expect that this parameter would be nearly constant within the measured area in Fig. 4. This supports the idea that the scatter of *St* is due to the heterogeneity of differential stress, *t*.

In lattice strain theory, the stress state is assumed to be uniform over the sample (Singh, 1993). In addition, microscopic deviatoric stresses may be present that manifest themselves as broadening of diffraction lines (Weidner, 1998). It is likely that both macro- and micro-scale stresses are present in our samples. The measured *St* values (Fig. 3) provide evidence of the former while narrowing of the diffraction peaks (by $\sim 20\%$) upon heating (Shim et al., 2000) provide evidence for the latter. In this study, we assume that the stress state is homogeneous over the volume sampled by our 10×10 μm X-ray probe.

The heterogeneity of the stress condition could have affected the earlier DAC studies for $CaSiO_3$ perovskite (Tamai and Yagi, 1989; Yagi et al., 1989; Tarrida and Richet, 1989; Mao et al., 1989) where a large X-ray beam size was used (60 μm, Yagi et al., 1989 and Mao et al., 1989, and 110 μm, Tarrida and Richet, 1989). The measurement over such a large volume containing heterogeneous stresses may explain the rather large random scatter of measured volumes for these earlier studies.

The uniaxial stress component, *t*, can be directly calculated for each *P*,*V* data point using the measured *St* value, provided that single-crystal elastic moduli are known as a function of pressure. For $CaSiO_3$ perovskite, these parameters have never been measured at high pressure or ambient pressure due to $CaSiO_3$ perovskite's instability at ambient conditions. The only available information on the single-crystal elastic stiffnesses, C_{ij}, of $CaSiO_3$ perovskite is the first principle calculation by Karki and Crain (1998). We calculated *S* using their result. According to this calculation, *S* is positive from ambient pressure to 140 GPa. This is consistent with our result that requires $S > 0$. No clear pressure dependence of *St* can be resolved by our data. The calculation of Karki and Crain (1998) suggests *S* decreases rather strongly with pressure. However, it is expected that *t* will increase with compression (Duffy et al., 1999a,b). Hence, the approximately constant value of *St* in Fig. 3 may be consistent with a decrease in *S* with compression.

However, if we use Karki and Crain's *S* value to calculate the uniaxial stress component, *t*, from *St*, the uniaxial stress component should be more than 15 GPa for the entire pressure range. This value is surprisingly high. If true, this implies that $CaSiO_3$ perovskite is an exceptionally strong material. However, uncertainty in the C_{ij}'s and *St* values makes these *t* values highly uncertain.

According to Fig. 3b, *St* of platinum is almost randomly scattered around zero with a slight positive sign (average value is 0.0023 ± 0.0052). The *S* of platinum is also unknown at high pressure. Thus, by

using our average St value and the calculated S at ambient condition from Macfarlane and Rayne (1965), the average t is estimated to be 0.7 GPa. However, for the maximum St observed for platinum ($St \sim 0.012$), the differential stress could be as large as 3.9 GPa.

One can expect that the differential stress could be reduced by using a soft pressure-transmitting medium. Thus, one might expect that argon might be better than NaCl as a pressure-transmitting medium. Interestingly, the St value from the experiment using an argon medium is not systematically smaller than that which used NaCl. Argon is known to freeze above 1.2 GPa at 300 K (Finger et al., 1981). The comparable sample St values with argon may indicate that the strength of solid argon is comparable to that of NaCl at high pressure. However, in terms of chemical inertness, argon is still better as a pressure-transmitting medium.

4.2. EOS of $CaSiO_3$ perovskite

Since differential stress can produce systematic error in measured volume and pressure, characterizing the uniaxial stress component is crucial to obtain an accurate P–V EOS curve. Ideally, we should have a hydrostatic stress state surrounding the sample to determine elastic properties by fitting the P–V data to an EOS. In other words, the P–V relationship should be measured where t is close to zero.

Fig. 5 shows the measured P,V points at 300 K. The St value for each data point is represented using a color scale. All measured points are shown including those measured at the heated spot and at nearby positions. As shown in Fig. 4a, the heated spot is not

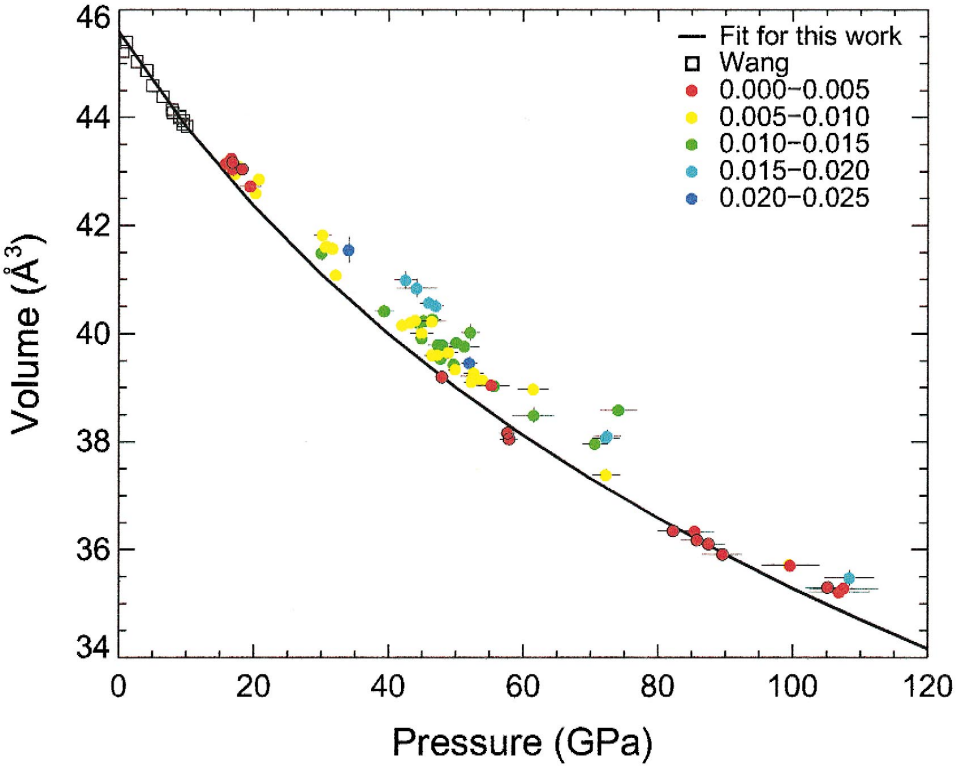

Fig. 5. Measured P,V data and EOS fit to the third-order Birch–Murnaghan EOS. The fit was performed for the points which have $|St| < 0.005$ (red circles) for both $CaSiO_3$ perovskite and platinum combined with data by Wang et al. (1996). The error bar represents the estimated uncertainty (1σ) of pressure and volume. Data points whose symbol has a black edge were used for EOS fitting.

Table 1
The data points used for EOS fitting. The number in parenthesis is estimated uncertainty (1σ)

Pressure (GPa)	Volume (Å^3)	Pressure medium
16.8(11)	43.167(58)	Ar
18.3(5)	43.044(28)	Ar
47.9(10)	39.194(36)	NaCl
57.7(12)	38.158(33)	Ar
57.9(13)	38.049(34)	Ar
82.3(22)	36.347(54)	Ar
85.8(24)	36.175(75)	Ar
87.5(25)	36.104(68)	Ar
89.6(30)	35.909(55)	Ar
105.2(33)	35.300(86)	Ar

necessarily the minimum *St* spot, although it generally shows a small *St* value.

Fig. 5 shows that there is a great deal of scatter in the *P*,*V* data points even when a pressure-transmitting medium is used. However, the points with similar *St* value, i.e., same color in Fig. 5, are aligned along bands in the *P*–*V* plane. It is clear that data points with low *St* yield lower volumes for a given pressure. The *St* value increases as one moves to increasing volumes at constant pressure. Hence, the larger differential stress results in a larger volume for a given pressure. This is consistent with the well-known behavior of DAC samples under non-hydrostatic stress (Kinsland and Bassett, 1977) and was also observed in radial diffraction experiments (Duffy et al., 1999a).

The generation of stress in a DAC is uniaxial. The X-ray beam passes near the axial direction of the DAC in the normal geometry, so that the X-rays only sample the d-spacing near the minimum stress direction. Under highly non-hydrostatic conditions, the volume would be significantly overestimated in this case. This effect will be greater if the shear strengths of the sample and pressure standard are different.

In the laser-heated diamond-anvil cell (LHDAC) experiment, platinum is normally used as both a pressure standard and laser absorption material. However, as shown above, the strength of platinum is relatively small. However, some silicates, i.e., $CaSiO_3$ perovskite as in this study, and oxides, MgO (Duffy et al., 1995; Shim and Duffy, unpublished data), should be able to sustain much larger differential stress. A $CaSiO_3$ perovskite–platinum mixture, such as used here, could be very sensitive to deviatoric stress.

To fit *P*,*V* data to the third order Birch–Murnaghan equation, data points were selected from our data set which have *St* value less than 0.005 both for $CaSiO_3$ perovskite and platinum (Table 1). The choice of $|St| < 0.005$ is justified by the fact that this corresponds to the range of *St* values found at high temperature (Shim et al., 2000). A total of 10 data points meet this criterion. These data points were presented in Fig. 3 using solid symbols.

Since we do not have data points below 15 GPa, V_0 cannot be constrained by the present data alone. We thus combined our data with the lower pressure data ($P \leq 10$ GPa) of Wang et al. (1996). The weighting factor for each data point was calculated using the experimental uncertainty in pressure and volume. By fitting to a third order Birch–Murnaghan equation, the isothermal bulk modulus of $CaSiO_3$ perovskite, K_{T0}, is found to be 236 ± 4 GPa and its pressure derivative, K'_{T0} is to be 3.9 ± 0.2 (Table 2). If K'_{T0} is fixed to 4.0, a value of K_{T0} equal to 234 ± 2 GPa results. These bulk modulus values are significantly lower than those of previous DAC measurements, but consistent with lower pressure measurements by Wang et al. (1996) and the first principles calculation by Karki and Crain (1998).

Table 2
EOS parameters for $CaSiO_3$ perovskite compared with previous studies. The number in parenthesis is the 1σ estimated uncertainty

	V_0 (Å^3)	K_{T0} (GPa)	K'_{T0}
This work	45.58 *	236(4)	3.9(2)
Theoretical calculations			
Wolf and Jeanloz (1985)	55.74	274	3.85
Hemley et al. (1987)	45.81	347	5.3
Sherman (1993)	44.96	300	4.0
Wentzcovitch et al. (1995)	46.15	254	4.4
Chizmeshya et al. (1996)	45.62	255.6	4.724
Karki and Crain (1998)	45.35	241	4.14
Experimental measurements			
Tamai and Yagi (1989)	45.58(7)	325(10)	4.0 *
Yagi et al. (1989)	45.58(7)	288(13)	4.0 *
Tarrida and Richet (1989)	45.60(10)	275(15)	4.0 *
Mao et al. (1989)	45.37(8)	281(4)	4.0 *
Wang et al. (1996)	45.58(4)	232(8)	4.8(3)

* Fixed parameter.

In earlier DAC studies, the data scatter precludes precise determination of the pressure derivative of the bulk modulus, K_0'. In the LVP study that covered a limited pressure range ($P \leq 10$ GPa), to obtain a constraint on K_{T0}', Wang et al. (1996) combined their data with the high-pressure DAC data of Mao et al. (1989). A large value of K_{T0}' ($=4.8$) was obtained by reconciling their data with Mao et al.'s (1989) non-hydrostatic measurement. The resultant compression curve of Wang et al. (1996) is not distinguishable from that of Mao et al. (1989) over the mantle pressure range where $CaSiO_3$ perovskite is stable.

To compare the scatter of data points in our study with previous studies, we overlay all available data sets in Fig. 6. Interestingly, the data scatter from this study is comparable to that of previous studies. The EOS of Mao et al. (1989) is generally consistent with our data points which have $St = 0.015$. This suggests that earlier studies such as Mao et al. (1989) are significantly affected by non-hydrostatic stress. However, our selected data points which have the smallest differential stress components indicate that the density and bulk modulus at lower mantle pressure and 300 K is 1–3% greater and 5–15% smaller, respectively, than those of previous studies (Tamai and Yagi, 1989; Yagi et al., 1989; Tarrida and Richet, 1989; Mao et al., 1989; Wang et al., 1996) (Fig. 6).

In combining different data sets, one needs to ensure that the stress conditions of sample are similar during the experiment. Wang et al. (1996) claimed that by heating the sample before measuring the 300 K XRD spectra they could decrease the non-hydrostatic stress to less than 0.05 GPa by watching the relative diffraction line shift of NaCl or BN, both of which existed in the sample capsule with $CaSiO_3$ perovskite. Thus, it is reasonable to combine our low

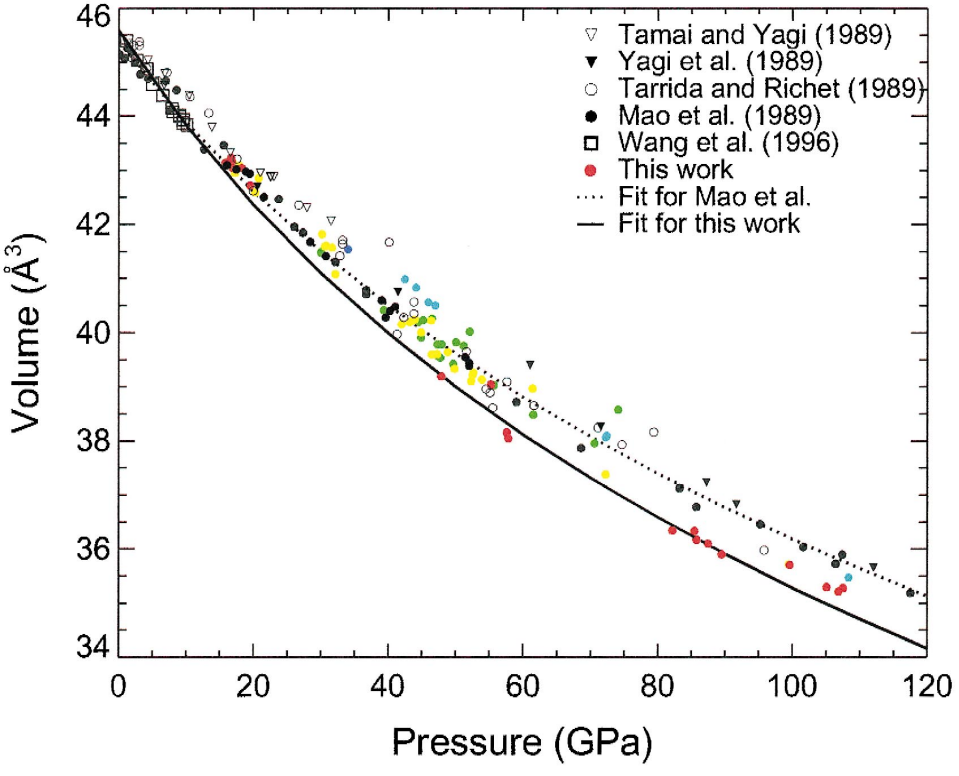

Fig. 6. P–V measurements from this study and previous studies (Tamai and Yagi, 1989; Yagi et al., 1989; Tarrida and Richet, 1989; Mao et al., 1989; Wang et al., 1996). The color scale for St values is the same as in Fig. 5.

St data with Wang et al.'s (1996) data since these are the only data sets for which a low deviatoric stress can be demonstrated.

In this study, *St* and volume calculations were performed for the cubic unit cell of $CaSiO_3$ perovskite. However, a tetragonal ($I4/mcm$) distortion of cubic ($Pm3m$) $CaSiO_3$ perovskite has been proposed based on theoretical calculations (Stixrude et al., 1996). This calculation suggests that the cubic phase is unstable compared to the tetragonal phase for all pressures at the ground state. We investigated the evidence for this by calculating the XRD pattern based on the proposed tetragonal structure. It turns out that the peak splitting for such a small distortion (0.7% change of c/a ratio) is close to the resolution limit of EDXD technique. Assuming 0.7% c/a ratio change for $CaSiO_3$ perovskite and 0.5 keV full width at half maximum (FWHM) for EDXD, however, the distortion should still result in selective peak broadening in the case of small splittings (e.g., cubic 200 and 110 lines) and the appearance of new peaks for larger splittings (e.g., cubic 111 line). These were not observed in any of our XRD measurements.

Nevertheless, if an undetectable tetragonal distortion exists with less than 0.7% c/a ratio change, this will affect the *St* calculation. However, our calculations show that the proposed distortion will yield only $St = 0.0008$. If we assumed even a 50% intensity change caused by preferred orientation, so the apparent centroids of nearly overlapped peaks are shifted, *St* can vary within only $-0.0007 \sim 0.0046$ range, which is much less than the observed *St* of $CaSiO_3$ perovskite. Thus, the observed *St* of $CaSiO_3$ perovskite cannot be explained by tetragonal distortion. Also, this distortion can result in $\pm 0.28\%$ change for the measured volume. Again, this is no more than the experimental uncertainty. If the magnitude of distortion is larger than the proposed one, we expect it would be detectable by EDXD.

5. Conclusion

XRD patterns were measured to 108 GPa for $CaSiO_3$ perovskite in the DAC. Argon or NaCl was used as pressure-transmitting media. By defining the product of the uniaxial stress component, *t*, and the elastic anisotropy, *S*, we can describe the stress condition of the sample under various conditions, such as after temperature quench and after cold compression. At a given pressure, the *St* value shows a large variation from 0.005 to 0.025. This indicates heterogeneity in the stress state for different positions in the sample.

Data points where a large non-hydrostatic stress component exists yield larger volumes for $CaSiO_3$ perovskite, whereas for points where the stress condition is close to hydrostatic the measured volume is relatively smaller. However, because the pressure standard, platinum, is less sensitive to deviatoric stress, this heterogeneous stress condition of the sample results in a large amount of scatter for measured volumes at the same pressure. This may have affected earlier DAC measurements where a large diameter X-ray beam was used and the stress conditions were not characterized.

It can be demonstrated that the data points and EOS fit to earlier DAC data by Mao et al. (1989) follow along a curve corresponding to a relatively high *St* value of 0.015 in the current study. By choosing the data points which have $St \leq 0.005$ for platinum and $CaSiO_3$ perovskite and combining with lower pressure data by Wang et al. (1996), we find that $CaSiO_3$ perovskite is much more compressible than found in earlier DAC or LVP studies. The fitting result is $K_{T0} = 236 \pm 4$ GPa and $K'_{T0} = 3.9 \pm 0.2$. The bulk modulus is much smaller than previous DAC measurements (Tamai and Yagi, 1989; Yagi et al., 1989; Tarrida and Richet, 1989; Mao et al., 1989) and is consistent with LVP measurements (Wang et al., 1996). However, the pressure derivative of the bulk modulus is significantly different from that of Wang et al. (1996) who relied on non-hydrostatic high-pressure measurements by Mao et al. (1989) in order to resolve K'_{T0}.

Our new compression curve indicates that the density and bulk modulus of $CaSiO_3$ perovskite are 1–3% greater and 5–15% smaller, respectively, at lower mantle pressures (25–135 GPa) at 300 K than previous studies. As Shim and Duffy (2000) point out, higher order thermoelastic parameters, which are obtained by fitting P–V–T data, are strongly affected by small uncertainties in the 300 K compression curve. Therefore, the improved 300 K EOS will enable us to better determine the density and bulk modulus $CaSiO_3$ perovskite at the lower mantle

pressure and temperature conditions, as discussed in a separate publication (Shim et al., 2000).

Acknowledgements

We thank Sergio Speziale and Abby Kavner for experimental assistance and T. Yagi and an anonymous reviewer for valuable comments. This research was supported by the NSF. Portions of this work were performed at GeoSoilEnviroCARS (GSECARS), Sector 13, Advanced Photon Source at Argonne National Laboratory. GSECARS is supported by the National Science Foundation–Earth Sciences, Department of Energy–Geosciences, W.M. Keck Foundation, and the United States Department of Agriculture. Use of the Advanced Photon Source was supported by the U.S. Department of Energy, Basic Energy Sciences, Office of Energy Research, under Contract No. W-31-109-Eng-38.

References

Chizmeshya, A.V.G., Wolf, G.H., McMillan, P.F., 1996. First-principles calculation of the equation-of-state, stability and polar optic modes of $CaSiO_3$ perovskite. Geophys. Res. Lett. 23, 2725–2728.

Duffy, T.S., Hemley, R.J., Mao, H.-K., 1995. Equation of state and shear-strength at multi-megabar pressures — magnesium oxide to 227 GPa. Phys. Rev. Lett. 74, 1371–1374.

Duffy, T.S., Shen, G., Heinz, D.L., Singh, A.K., 1999a. Lattice strains in gold and rhenium under non-hydrostatic compression to 37 GPa. Phys. Rev. B: Condens. Matter Mater. Phys., in press.

Duffy, T.S., Shen, G., Shu, J., Mao, H.-K., Hemley, R.J., Singh, A.K., 1999b. Elasticity, shear strength and equation of state of molybdenum and gold under non-hydrostatic compression to 24 GPa. J. Appl. Phys. 86, 6229–6736.

Finger, L.W., Hazen, R.M., Zou, G., Mao, H.-K., Bell, P.M., 1981. Structure and compression of crystalline argon and neon at high pressure and room temperature. Appl. Phys. Lett. 39, 892–894.

Hemley, R.J., Jackson, M.D., Gordon, R.G., 1987. Theoretical study of the structure, lattice dynamics, and equations of state of perovskite-type $MgSiO_3$ and $CaSiO_3$. Phys. Chem. Miner. 14, 2–12.

Hirose, K., Fei, Y., Ma, Y.Z., Mao, H.-K., 1999. The fate of subducted basaltic crust in the Earth's lower mantle. Nature 397, 53–56.

Holmes, N.C., Moriarty, J.A., Gathers, G.R., Nellis, W.J., 1989. The equation of state of platinum to 660 GPa (6.6 Mbar). J. Appl. Phys. 66, 2962–2967.

Karki, B.B., Crain, J., 1998. First-principles determination of elastic properties of $CaSiO_3$ perovskite at lower mantle pressures. Geophys. Res. Lett. 25, 2741–2744.

Kinsland, G.L., Bassett, W.A., 1977. Strength of MgO and NaCl polycrystals to confining pressures of 250 kbar at 25°C. J. Appl. Phys. 48, 978–985.

Liu, L., Ringwood, A.E., 1975. Synthesis of a perovskite-type polymorph of $CaSiO_3$. Earth Planet. Sci. Lett. 14, 209–211.

Macfarlane, R.E., Rayne, J.A., 1965. Anomalous temperature dependence of shear modulus c_{44} for platinum. Phys. Lett. 18, 91–92.

Mao, H.-K., Yagi, T., Bell, P.M., 1977. Mineralogy of the earth's deep mantle: quenching experiments on mineral compositions at high pressure and temperature. Carnegie Inst. Washington, Year Book 76, 502–504.

Mao, H.-K., Chen, L.C., Hemley, R.J., Jephcoat, A.P., Wu, Y., 1989. Stability and equation of state of $CaSiO_3$-perovskite to 134 GPa. J. Geophys. Res. 94, 17889–17894.

Mao, H.-K., Shu, J., Shen, G., Hemley, R.J., Li, B., Signh, A.K., 1998. Elasticity and rheology of iron above 220 GPa and the nature of the earth's inner core. Nature 396, 741–743.

Oguri, K., Funamori, N., Sakai, F., Kondo, T., Uchida, T., Yagi, T., 1997. High-pressure and high-temperature phase relations in diopside $CaMgSi_2O_6$. Phys. Earth Planet. Inter. 104, 363–370.

Rivers, M.L., Duffy, T.S., Wang, Y., Eng, P.J., Sutton, S.R., Shen, G., 1998. A new facility for high-pressure research at the Advanced Photon Source. In: Manghnani, M.H., Yagi, T. (Eds.), Properties of Earth and planetary materials at high pressure and temperature. Geophys. Monogr. 101 American Geophysical Union, pp. 79–87.

Shen, G., Mao, H.-K., Hemley, R.J., Duffy, T.S., Rivers, M.L., 1998. Melting and crystal structure of iron at high pressures and temperatures. Geophys. Res. Lett. 25, 373–377.

Sherman, D.M., 1993. Equation of state, elastic properties, and stability of $CaSiO_3$ perovskite: first principles (periodic Hartree–Fock results). J. Geophys. Res. 98, 19795–19805.

Shim, S.-H., Duffy, T.S., 2000. Constraints on the $P-V-T$ equation of state of $MgSiO_3$ perovskite. Am. Mineral. 85, 354–363.

Shim, S.-H., Duffy, T.S., Shen, G., 2000. The stability and $P-V-T$ equation of state for $CaSiO_3$ perovskite in the earth's lower mantle. J. Geophys. Res., in press.

Singh, A.K., 1993. The lattice strains in a specimen (cubic system) compressed nonhydrostatically in an opposed anvil device. J. Appl. Phys. 73, 4278–4286.

Singh, A.K., Mao, H.-K., Shu, J., Hemley, R.J., 1998. Estimation of single-crystal elastic moduli from polycrystalline X-ray diffraction at high pressure: application to FeO and iron. Phys. Rev. Lett. 80, 2157–2160.

Speziale, S., Zha, C.-S., Duffy, T.S., Hemley, R.J., Mao, H.-K., 2000. Quasi-hydrostatic compression of magnesium oxide to 52 GPa: implications for the pressure–volume–temperature equations of state. J. Geophys. Res., submitted for publication.

Stixrude, L., Cohen, R.E., Yu, R., Krakauer, H., 1996. Prediction

of phase transition in $CaSiO_3$ perovskite and implications for lower mantle structure. Am. Mineral. 81, 1293–1296.

Tamai, H., Yagi, T., 1989. High-pressure and high-temperature phase relations in $CaSiO_3$ and $CaMgSi_2O_6$ and elasticity of perovskite-type $CaSiO_3$. Phys. Earth Planet. Inter. 54, 370–377.

Tarrida, M., Richet, P., 1989. Equation of state of $CaSiO_3$ perovskite to 96 GPa. Geophys. Res. Lett. 16, 1351–1354.

Wang, Y., Weidner, D.J., Guyot, F., 1996. Thermal equation of state of $CaSiO_3$ perovskite. J. Geophys, Res. 101, 661–672.

Weidner, D.J., 1998. Rheological studies at high pressure. In: Hemley, R.J. (Ed.), Ultrahigh-pressure mineralogy — physics and chemistry of the earth's deep interior. Rev. Mineral. 37 Mineralogical Society of America, pp. 493–524.

Wentzcovitch, R.M., Ross, N.L., Price, G.D., 1995. Ab initio study of $MgSiO_3$ and $CaSiO_3$ perovskites at lower-mantle pressures. Phys. Earth Planet. Inter. 90, 101–112.

Wolf, G.H., Jeanloz, R., 1985. Lattice dynamics and structural distortions of $CaSiO_3$ and $MgSiO_3$ perovskite. Geophys. Res. Lett. 12, 413–416.

Yagi, T., Kusanagi, S., Tsuchida, Y., Fukai, Y., 1989. Isothermal compression and stability of perovskite-type $CaSiO_3$. Proc. Jpn. Acad., Ser. B 65, 129–132.